World Academy of Science, Engineering and Technology
International Journal of Civil and Environmental Engineering
Vol:17, No:3, 2023

Study of the Flow Structure in a Penstock in Unsteady Regime

F. Nkontchou Ngongang, M. Tchawe Tchawe, B. Djeumako, B. Kenmeugne

***Abstract*—**In this work, the flow structure in the Songloulou dam, is visualized in a time interval to observe the different fluid layers in our structure. Firstly, the three-dimensional modelling of the penstock is carried out in the software Gambit, followed by calculations in Fluent that proceeds introduction of boundary conditions. After calculation, we identified four periods corresponding to four regimes. In the first, spanning from 0.00 to 1.50s, we have the non-developed hydraulically rough turbulent regime, characterized by abrupt variations with modifications of the velocity fields. The second extends from 1.50 to 3.50s, where we have the transition regime characterized by slight variations and modifications of the velocity fields but with a great difference of the values of the current lines. From 3.50 to 5.00s, we encounter the third, which is the fully developed turbulent hydraulically rough regime, characterized by fields that vary no more, but have minute differences in the streamlines. The last period is from 5.00s and more, where we have a flow that is almost stationary, hence there are no changes in the fields.

***Keywords*—**Unsteady flow, penstock, friction coefficient, hydroelectric dam.

I. Introduction

HYDROELECTRIC dams are structures built across rivers to convert hydraulic energy into electrical energy. This process first involves the conversion of hydraulic energy into kinetic energy, which takes place in the penstock where many physical phenomena often originate. A conduit under pressure, called the penstock, is one of the most important elements in a hydroelectric power plant. It is located between the dam and the turbine. Its role is to convert the potential energy possessed by the water mass in the reservoir into kinetic energy, which will then be converted into mechanical energy by the turbine [1]. At this stage, the water velocities in the pipe change according to the layout of the pipe. The constant change of velocity and pressure causes instabilities when we consider that penstocks are also subject to internal pressures. These instability problems have become one of the main control conditions in the design of penstocks [2].

Cameroon currently has three large hydroelectric dams, including the Songloulou hydroelectric dam. With a total installed capacity of 384 MW, the Songloulou plant is currently the most powerful in Cameroon [3]. The study of flow in penstocks is necessary for the understanding of physical phenomenon present in order to facilitate maintenance and even its efficiency. Concerning the Songloulou dam penstock, very few studies have been conducted [4], [5].

We are interested in this work in the velocity fields met in-there, so we can understand the related changes. The main objective of this article is to visualize the flow structure within a time interval, with the purpose of locating the different structures of the flow in our edifice. To achieve this, we will make a three-dimensional modelling of the pipe to observe the variation of the fields. The main tool used is the CFD, which also offers the possibility of modelling three-dimensional flows, helping to understand complex phenomena [6].

II. Materials and Methods

A. Study Area

The penstock studied is that of the Songloulou hydroelectric dam. It is composed of two sections, which are our main study areas. Fig. 1 shows us the mesh of our conduit.

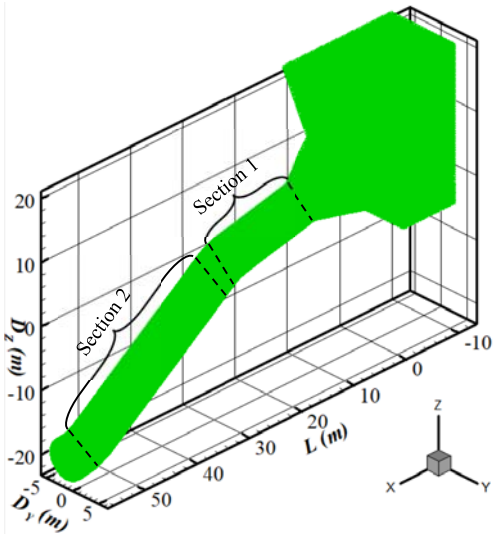

Fig. 1 Mesh of the three-dimensional domain of our pipe

The turbulence model used is the Renormalization Group (RNG) k-ε because it is well suited to boundary layers with a strong adverse pressure gradient [7], high curvature and vortex flows and considered isotropic. The second-order equations are solved with the SIMPLE (Semi Implicit Method for Velocity

F. Nkontchou Ngongang is with the Department of Mechanical Engineering of the ENSAI, University of Ngaoundere, CO 455 Ngaoundere Cameroon (corresponding author, phone: (+237) 674-768-612; e-mail: francois.nkontchou@gmail.com).

M. Tchawe Tchawe and B. Djeumako are with the Department of Mechanical Engineering of the ENSAI, University of Ngaoundere, CO 455 Ngaoundere-Cameroon (e-mail: christophetchawe88@gmail.com, djeumakob@gmail.com).

B. Kenmeugne is with the Department of Mechanical Engineering of the ENSPY, University of Yaounde 1, CO 8390 Yaounde-Cameroon (e-mail: kenmeugneb@gmail.com).

Linked Equations) velocity-pressure coupling method. The convergence criterion was fixed at 10^{-6} to increase the accuracy of the results [8].

B. Governing Equations

The governing equations for turbulent hydrodynamic flows are the conservation laws of mass, momentum and energy. The flow in our case is considered isothermal and the fluid is assumed Newtonian. The flow is incompressible, has a constant viscosity and can be described by the velocity and pressure field governed by the Navier-Stokes equations [6]-[8].

$$\frac{\partial(\rho\overline{u_i})}{\partial x_j} = 0 \tag{1}$$

$$\frac{\partial(\rho\overline{u_i}\overline{u_j})}{\partial x_j} = \frac{\partial p}{\partial x_i} + \frac{\partial}{\partial x_j}\left[\mu\left(\frac{\partial\overline{u_i}}{\partial x_j} + \frac{\partial\overline{u_j}}{\partial x_i} - \frac{2}{3}\delta_{ij}\frac{\partial\overline{u_l}}{\partial x_i}\right)\right] + \frac{\partial(\rho\overline{u_i'u_j'})}{\partial x_j} \tag{2}$$

where $(\overline{(\rho u_j' u_i')})$ is the Reynolds tensor, ρ the constant density, p is the static pressure load, u_i represents the velocities in x_i coordinate directions and μ the viscous stress.

Equation (1) is the continuity equation and (2) is the conservation of motion equation:

- The term on the left represents the convective transport term;
- The first term on the right side represents the forces generated by pressure;
- The second term on the right side represents the viscosity forces;
- The last term on the right side represents the forces generated by turbulence.

To solve these equations, we used a discretization scheme to transform the partial derivatives into an algebraic system of equations. When applied inside the geometry under constraints, these give the spatio-temporal variations of the system's quantities.

The standard integral form of the Navier-Stockes equation in a control volume V_p of center P is described as:

$$\int_t^{t+\Delta t}\left(\underbrace{\frac{d}{dt}\int_{V_p}\bar{u}dV}_{\text{dérivée temporelle}} + \underbrace{\int_{V_p}\nabla.(\bar{u}\bar{u})dV}_{\text{convection}} - \underbrace{\int_{V_p}\nabla.V_{eff}(\nabla u + \nabla u^T)dV}_{diffusion}\right)dt = -\int_t^{\Delta t}\left(\frac{1}{\rho}\underbrace{\nabla\bar{p}dV}_{\text{sources}}\right)dt \tag{3}$$

$\bar{u}$ and $\bar{p}$ are the filtered velocity and pressure, respectively, V_{eff} is the sum of the kinematic viscosity and the submesh turbulent viscosity.

The convective term can be rewritten as follows:

$$\int_{V_p}\nabla.(\bar{u}\bar{u})dV = \int_{\partial V}(\bar{u}\bar{u}).dS = \sum_{\mathcal{S}} S.\overline{u_{\mathcal{S}}}.\overline{u_{\mathcal{S}}} = \sum_{\mathcal{F}}\left(S.\overline{u_{\mathcal{S}}}^{n+1}\right).\overline{u_{\mathcal{S}}}^{n+1} \tag{4}$$

The flux through the surface $\mathcal{S}$, $\mathcal{F} = S.\overline{u_{\mathcal{S}}}$, used to solve for the velocity at the new time step, n+1, is that calculated from the velocity at the previous time step n. The value of the velocity at the face S is obtained by:

$$\bar{u}_{\mathcal{S}} = \mathcal{S}_x\bar{u}_p + (1-\mathcal{S}_x)\bar{u}_N \tag{5}$$

where $\mathcal{S}_x$ is the linear interpolation factor defined as the ratio of distances.

The sub-mesh model used introduces a sub-mesh viscosity that can be associated with the classical diffusion term. Let the stress tensor $\mathbb{B}$ be such that:

$$\mathbb{B} = \nu(\nabla.\bar{u} + \nabla.\bar{u}^T) + \tau = (\nu + \nu_{sm})(\nabla.\bar{u} + \nabla.\bar{u}^T) = \nu_{eff}(\nabla.\bar{u} + \nabla.\bar{u}^T) \tag{6}$$

where ν_{eff} is the effective viscosity in which the submesh viscosity is included. The two gradients are discretized separately.

The transpose of the velocity gradient for time n + 1 is calculated using the velocity at time n:

$$\int_{V_p}\nabla.\mathbb{B}dV = \int_{V_p}\nabla.\left[\nu_{eff}(\nabla.\bar{u} + \nabla.\bar{u}^T)\right]dV = \sum_{\mathcal{S}}\left(\nu_{eff}\right)_{\mathcal{S}} S.(\nabla.\bar{u})_{\mathcal{S}} + \nabla\left[\nu_{eff}(\nabla.\bar{u})^T\right] \tag{7}$$

The velocity gradient at the $\mathcal{S}$ face, $(\nabla.\bar{u})_{\mathcal{S}}$, is calculated by (5). The time variations of u and its integration in time can be written as:

$$\left(\frac{\partial\bar{u}}{\partial t}\right)_p = \frac{\bar{u}_p^{n+1} + \bar{u}_p^n}{\Delta t}$$
$$\int_t^{t+\Delta t}\bar{u}(t)dt = \frac{1}{2}(\bar{u}^n + \bar{u}^{n+1})\Delta t \tag{8}$$

where $\bar{u}^n$ andt $\bar{u}^{n+1}$ represent the filtered velocities at times n and $n+1$, respectively. This time discretization scheme is second order centred. These equations were solved in FLUENT [9].

III. Results and Discussion

A. Boundary Condition

The penstock of the Songloulou dam consists of two straight sections and two bends. The inlet of section 1 represents the inlet of the penstock and the outlet of section 2 represents the outlet of the penstock. The legends presented correspond to the average values existing in the whole structure, which can be higher or lower depending on the chosen position.

Table I gives us the parts of our structure with the boundary conditions that have been imposed to solve our different equations. The selected time step is 0.01 second.

TABLE I
Boundary Conditions

Part	Conditions
Inlet	Inlet velocity
Outlet	Outflow velocity
Pipe wall	Wall
Upstream water surface	Symmetric

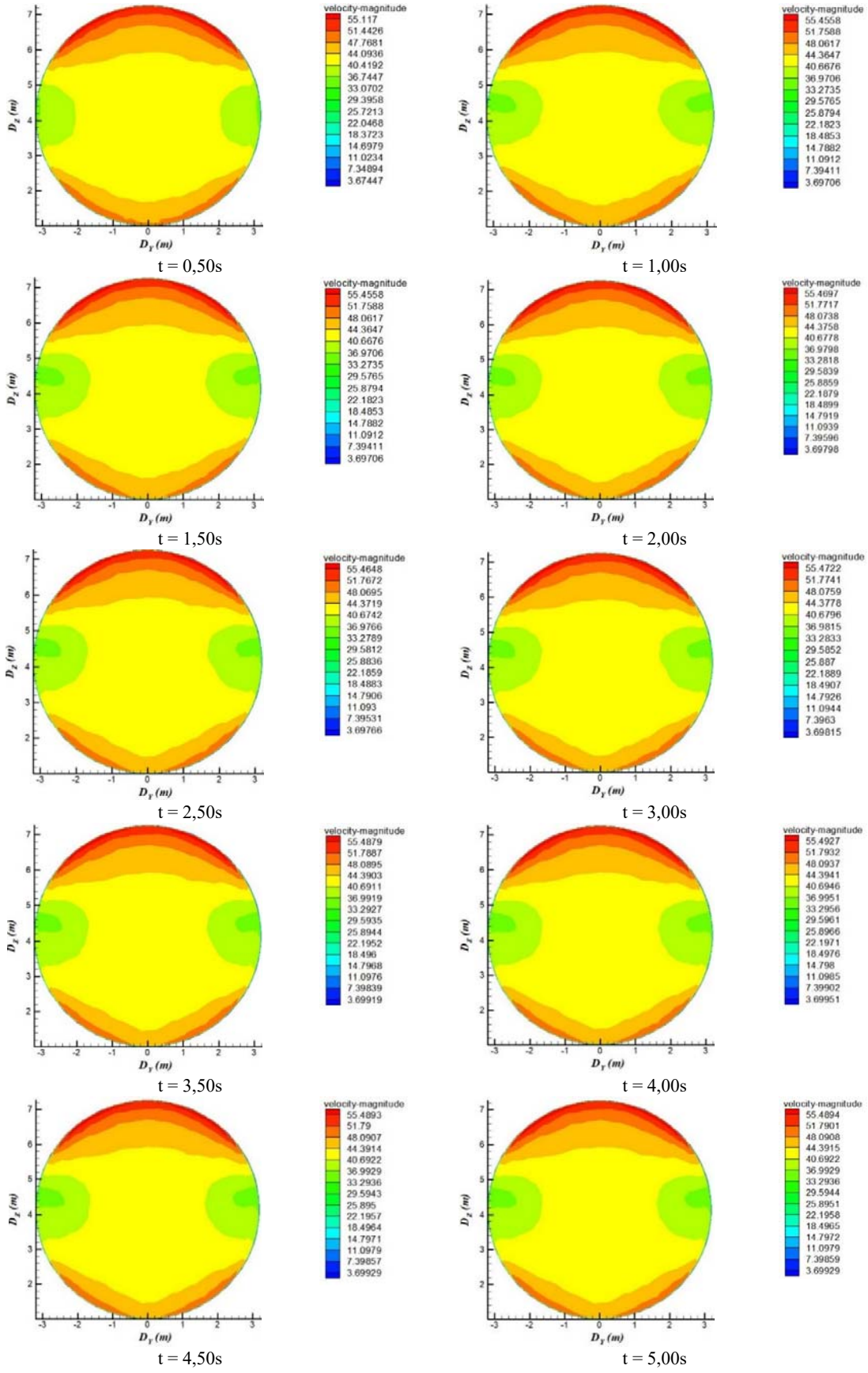

Fig. 2 Inlet to Section 1

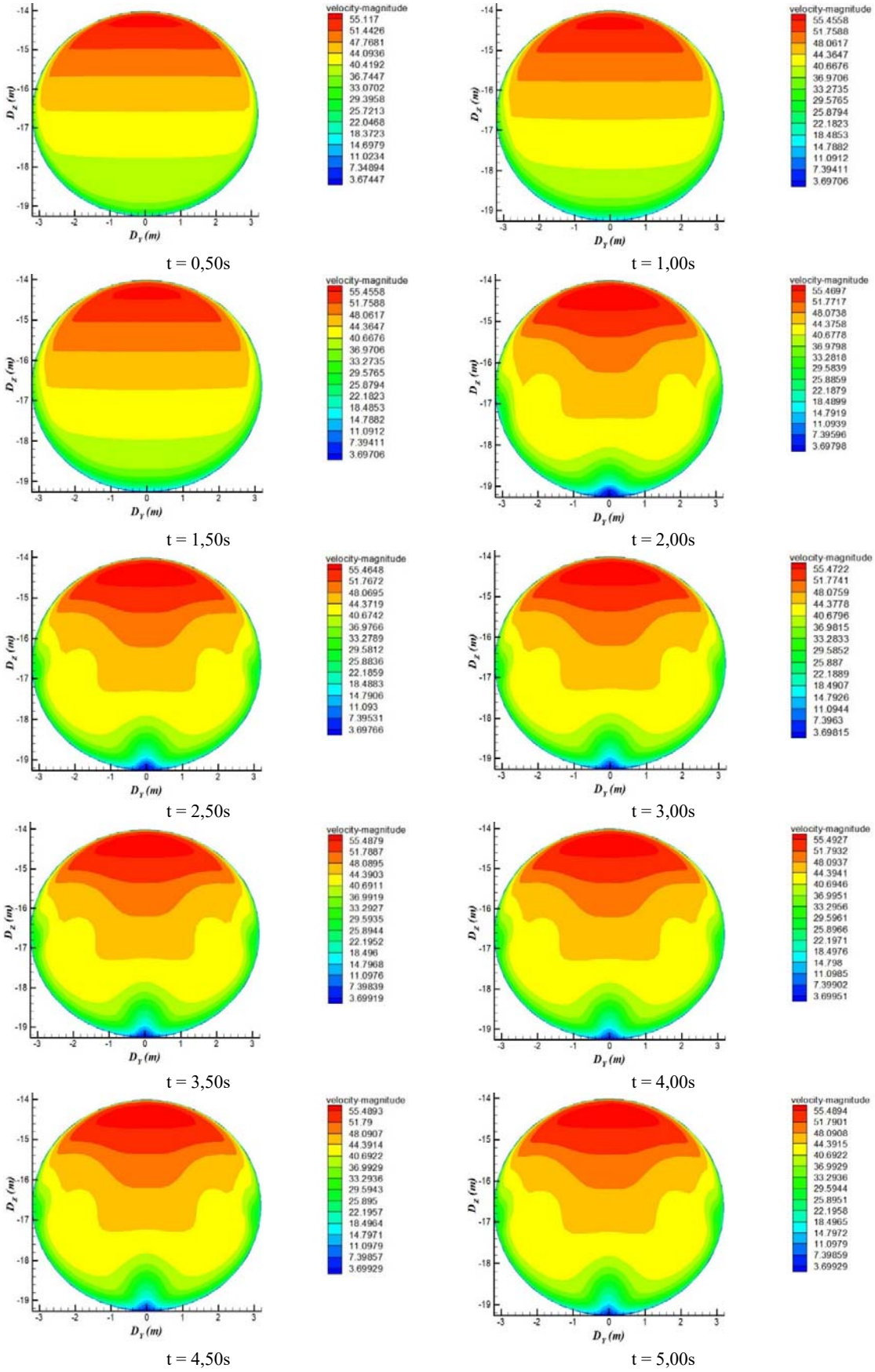

Fig. 3 Outlet of Section 2

B. Evolution of the Velocity Fields

1. Inlet of Section 1

Fig. 2 shows us the evolution of the velocity field in the section of the inlet of the penstock with pipe of roughness 0.05 for the average Reynolds value (Re = 28.8 x 10^6).

For the different times, the flow structure does not change. This is due to the upstream flow of the intake dam. In this part of the dam the streamlines are not influenced by time. The flow is uniform and considered macroscopically stationary due to the dimensional parameters of the river. The intake is the part that connects the inlet of Section 1 to the intake dam. It also has very large dimensions in all three directions in relation to the penstock. Therefore, the flow keeps the same structure over time, but the streamline values increase.

2. Outlet of Section 2

We also present in Fig. 3, the velocity fields at the outlet of Section 2.

At the outlet of section 2, the flow does not keep the same structure over time as we saw at the inlet. During the first seconds, i.e. until t = 1.50s, the flow keeps the same structure with the current lines orthogonal to the axes. The velocity fields are parallel and easily identifiable with visible boundaries marking the changes in values. Just after t = 1.50s, we observe an abrupt change in the flow structure with the onset of boundary layer detachment on the low wall. In the whole penstock, it is in this section that we have the highest velocities. As the velocity reaches its maximum in this section, we also observe the greatest detachment from the wall.

C. Velocity Profile

For each instant considered, we plot the corresponding velocity profiles. Figs. 4 and 5 show the evolution of velocity over time at the inlet and the outlet of the penstock.

We have a distribution at the entrance of the pipe that is almost symmetrical, because at this level the impact of the pipe's inclination is not yet felt. We see on the upper wall a rather fast detachment of the boundary layer, which on the lower wall is not visible. The non-detachment on the low wall is caused by friction forces that are very negligible compared to the forces created by the kinematic energy recovered by the fluid in the inlet. Whatever the time, the profiles are similar and even merge, reflecting the shape of the flow upstream. We have in the intake a flow that can be considered stationary because the velocity variations are not visible. On the other hand, at the outlet of the penstock, we have profiles that differ over time as shown in Fig. 5.

Until 1.00s, a linear distribution in the section is seen. After this time, this profile starts to change progressively to 1.50s. After this period, we observe a phenomenon of velocity drop in the lower part of the conduit. In the lower part of the penstock, the recirculation phenomenon actually starts from t = 2.00s. This phenomenon occurs between 1 m and 2 m from the bottom wall. In this interval, we have negative velocities.

Following the analysis proposed by [10], we can divide over time the different phases that we have in the flow structure of our penstock.

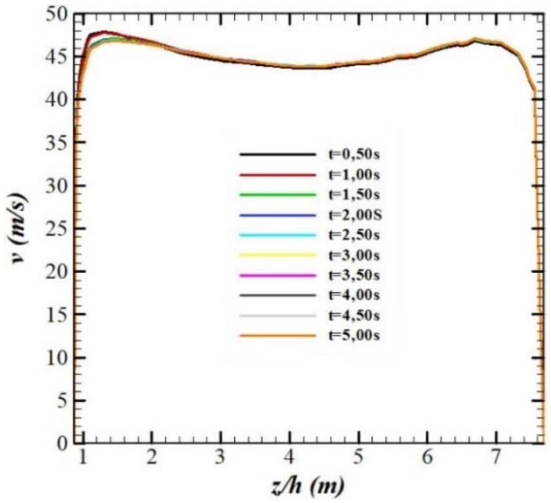

Fig. 4 Velocity profile at the inlet of the penstock

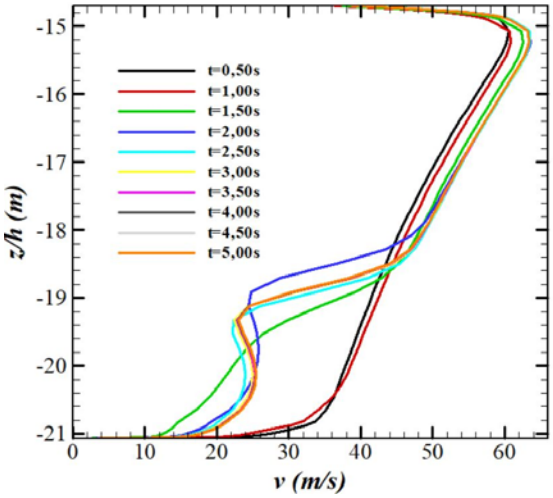

Fig. 5 Velocity profile at the outlet of the penstock

TABLE II
FLOW REGIMES IN THE PENSTOCK

Period	Regime	Characteristic
0.00s to 1.50s	Non-developed turbulent	Consistency of field and profile variations
1.50s to 3.50s	Transient	Small variations and different current lines
3.50s to 5.00s	Fully developed hydraulically rough turbulent	Uniform field and profile and slight differences in current line variations
5,00s and more	Turbulent stationary	Field and current line variations are negligible

D. Comparative Studies

Wang et al. [11] evaluated the accuracy of the flowmeter installed on the Three Gorges Dam, performing an experimental work and a numerical work to validate the former. Tchawe et al. [12] studied the flow upstream the Songloulou dam and in the intake in steady state. They explain the instability problem in the flow caused by the presence of the weir at the inlet of the intake. Fig. 6 highlights the profiles they obtained and ours in the penstock. Thus, we observe that by progressing inside the pipe, the flow tends to be symmetrical. The maximum velocity

is observed near the walls as shown in Fig. 6. Having worked in an unsteady regime, we observe approximately the same structure whatever the time considered at the same position. In the same logic, we brought out the velocity fields in order to observe the behaviour of the fluid layers in well-defined sections of the penstock. To do so, we considered the studies of Adamkowski et al. [13] who visualized the velocity fields in a curved pipe by a numerical approach to determine the form factor as shown in Fig. 7 (a).

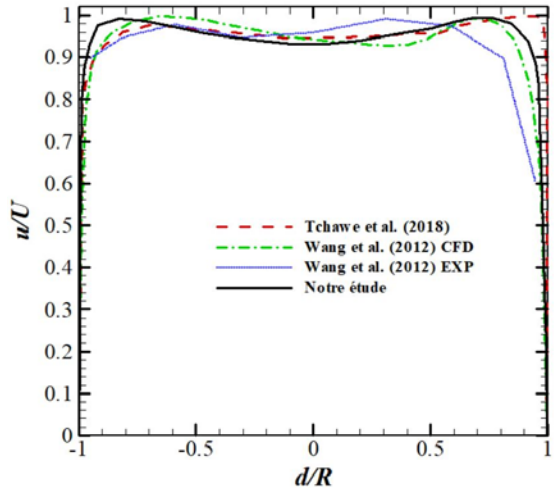

Fig. 6 Flow structure in the transverse direction

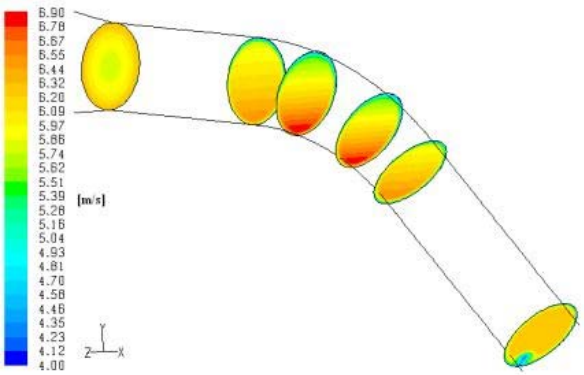

Fig. 7 (a) Velocity fields in the penstock for Adamkowski et al. [13]

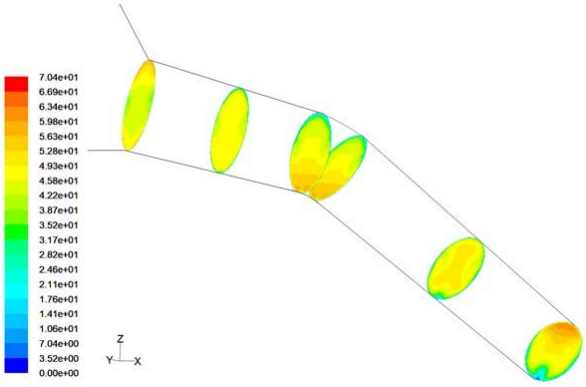

Fig. 7 (b) Velocity fields in the penstock for our study

We observe a consistency on the flow structure in all key parts of the pipe with a symmetry along the vertical in the fields, as also observed by Adamkowski et al. [13]. At the outlet, we have the high velocities on the upper wall and a pronounced detachment on the lower wall as observed in the work done by Adamkowski et al. [13].

IV. Conclusion

In this work, we visualized the flow structure in a time interval in order to observe the different fluid layers in our structure. To achieve this, we made a three-dimensional modelling of the penstock to observe the variation of the fields in the three directions. The study is carried out in unsteady regime and the considered times go from t = 0.50s to t = 5.00s. After calculation, we classified the phases in our flow into four categories that correspond to the four phases present. These phases have each their own characteristics. We have an undeveloped turbulent regime, a transient regime, a fully developed hydraulically rough turbulent regime and a turbulent regime that can be treated as stationary. This fourth phase reflects the fact that after 5.00s, the variations of velocity and pressure can be considered as negligible.

References

[1] R. Kumar and Singal, "Penstock material selection in small hydropower plants using MADM methods," *Renewable and Sustainable Energy Reviews*, vol. 52, pp 240–255, 2015.

[2] D. Wensheng, L. Xuemei and L. Yunhua, "Analysis of Stiffened Penstock External Pressure Stability Based on Immune Algorithm and Neural Network," *Hindawi Publishing Corporation Mathematical Problems in Engineering*, vol 14, Article ID 823653, 11 p., (2014)

[3] M. G. Ftatsi, T. Larrard and F. Duprat, "Fiabilité fonctionnelle résiduelle d'un barrage atteint de réaction alcali-granulats," *AJCE*, vol 36, Issue 1, pp. 84 – 87, (2018).

[4] T. Tchawe, D. Tcheukam-Toko., N. Kenmeugne and T. Djiako, "Numerical Study of Flow in the Water Inlet of the Penstock of a Hydroelectric Dam," *International Journal of Current Research*, vol. 10, Issue 07, pp. 71061-71066, (2018).

[5] F. Nkontchou, T. Tchawe, Tientcheu N., T. Djiako, B. Djeumako and D. Tcheukam-Toko, "Determination of the Dynamic Field in the Penstock of the Trois-Gorges Dam by a Numerical Approach," *International Journal of Energy Engineering*, 2021,11(1): 9-16

[6] D. Wilson, "Turbulence modeling for CFD," DCV industries, 2nd Edition, 1998.

[7] D. Bates, N. Lane and I. Ferguson, "Computational Fluid Dynamics: Applications in Environmental Hydraulics," *John Wiley & Sons, Ltd*, ISBN: 0-470-84359-4, (2005).

[8] T. Von Karman, "The fundamentals of the statistical theory of turbulence," *Journal of Aeronautical Science*, vol 4, 131-138, (1984).

[9] Fluent, User manual 6.3.26, (2006).

[10] D. Brkic and P. Praks, "Unified Friction Formulation from Laminar to Fully Rough Turbulent Flow," *Applied Sciences MDPI*, vol 8, no 2036 (2018); doi :10.3390/app8112036

[11] C. Wang, T. Meng, H. Hu and L. Zhang, "Accuracy of the ultrasonic flow meter used in the hydroturbine intake penstock of the Three Gorges Power Station," *Flow Measurement and Instrumentation*, vol 25, pp 32–39 (2012).

[12] T. Tchawe, T. Djiako, B. Kenmeugne and D. Tcheukam-Toko, (2018), "Numerical Study of the Flow Upstream of a Water Intake Hydroelectric Dam in Stationary Regime," *American Journal of Energy Research*, vol 6, No. 2, pp 35-41, 2018.

[13] A. Adamkowski, Z. Krzemianowski and W. Janicki, "Improved Discharge Measurement Using the Pressure-Time Method in a Hydropower Plant Curved Penstock," *Journal of Engineering for Gas Turbines and Power*, vol 131, 6 p, 2009.